International Journal of Engineering, Mathematical and Physical Sciences
ISSN: 2517-9934
Vol:8, No:5, 2014

Stimulus-Dependent Polyrhythms of Central Pattern Generator Hardware

Le Zhao, Alain Nogaret

***Abstract*—**We have built universal central pattern generator (CPG) hardware by interconnecting Hodgkin-Huxley neurons with reciprocally inhibitory synapses. We investigate the dynamics of neuron oscillations as a function of the time delay between current steps applied to individual neurons. We demonstrate stimulus dependent switching between spiking polyrhythms and map the phase portraits of the neuron oscillations to reveal the basins of attraction of the system. We experimentally study the dependence of the attraction basins on the network parameters: The neuron response time and the strength of inhibitory connections.

***Keywords*—**Central pattern generator, winnerless competition principle.

I. Introduction

CENTRAL pattern generator (CPG) are small groups of neurons that can generate rhythmic motor patterns, such as breathing, chewing, and locomotor movements without patterned sensory input [1]-[3]. Experiments have shown that CPG is a nonlinear network made of multiple coupled neurons whose output is spatiotemporal oscillations [4], [5]. Rhythmic burst is produced via the interaction between neurons such as excitatory, or gap junction synapses when the network is activated [6]. Theory shows that a system of three neurons possesses five stable rhythmic patterns corresponding to neurons firing in a sequence of two neurons firing in phase and out of phase with the third. Whether the system converges to one mode of oscillations or another depends on the initial conditions defined by the relative timing of the current steps stimulating the neurons [7]. Wojcik et al have mapped the basins of attraction of the 3 neuron central pattern generator [7]. Here we build a neural network with three Hodgkin-Huxley silicon neurons [8]. Neurons are connected via mutually inhibitory gap junction synapses with asymmetric conductance. We find that two different spatiotemporal patterns are generated by our neural circuit in the steady-state. These systems can be made to switch between these two patterns depending on the choice of the initial conditions represented by the relative timing of the current stimuli.

We use winnerless competition principle (WLC) [9], [10] to explain the dynamics in our neural network. Electrical activity bounces from one neuron to the next in the winnerless network according to a certain sequence determined by the strength of the inhibitory connections between neurons. When individual neurons are stimulated by a current step, a transient interval occurs during which the spiking patterns are not periodic. For different initial conditions, the spiking patterns evolve towards a steady state regime which is a limit cycle in a three dimensional plot and which strongly depends on initial conditions. Here we map the transient dynamics of the experimental CPG and show that stable attractors can be identified in a phase lag map. These spatiotemporal oscillations representing these attractors are important as they have been predicted to form memory states of networks of winnerless networks [11].

L. Zhao is with the Department of Physics, Bath, The U. K. (phone: +44-01225-385385; e-mail: lz304@ bath.ac.uk).

A. Nogaret is with the Department of Physics, Bath, The U. K., (phone: +44-01225-385609; e-mail: a.r.nogaret@bath.ac.uk).

II. Method

We made a network with 3 analogue neurons (Fig. 1). Our neurons model the NaKl Hodgkin-Huxley equations [8]. The neurons replicate the dynamics of ion channels and are used here because they are the most physiologically meaningful which is important for neurostimulation [13]. These neurons are versatile in that it is possible to include additional ion channels to describe the complex dynamics associated with the Calcium (L, T) currents or currents in real neurons. Finally, the parameter space of these neurons is quite large which is important to "program" them to replicate to the identical the dynamics of biological CPGs. Further analogue neurons present the advantages of computing in real time without the limitation on accuracy of software neurons [14]. The 'membrane' voltage of artificial neurons oscillates between the 0V and the 3.7V levels which are the analogues of the Na action potential (+50mV) and the K action potential (-70mV) in real neurons. The activation and inactivation voltage thresholds of the Na and K ion channels were set by scaling the known biological thresholds to the 0-3.7V interval [15].

The frequency of the spiking patterns was determined by the time constants of the Na and K gates together with the 'membrane' capacitance. We vary the frequency in the range between 357Hz and 714Hz to study the dependence of attraction basins on the spiking frequency.

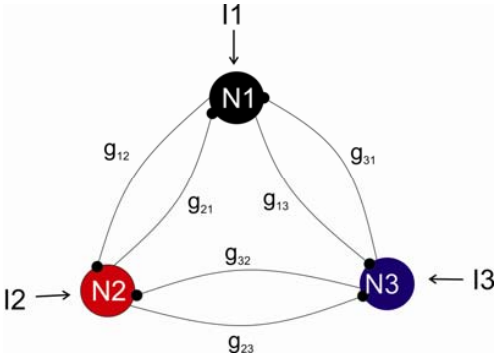

Fig. 1 Network with 3 neurons. Neurons compete with each other for firing due to the inhibitory synapse connection. The firing sequence is determined by both coupling strengths (the values of g_{12}, g_{21}, g_{13}, g_{31}, g_{23}, g_{32}) and the current stimulus (I1, I2, and I3)

The neurons are inhibitory connected by gap junction synapses, which are implemented using the VLSI differential current amplifiers shown in Fig. 2 [12]. The conductance of the synapse can be obtained from the equation below:

$$I_{out} = g(V_{\max})(V_1 - V_2) \quad (1)$$

Thus

$$g(V_{\max}) = \frac{I_{out}}{V_1 - V_2} \quad (2)$$

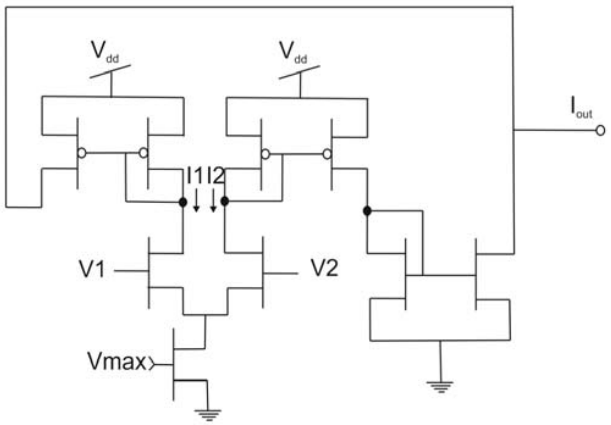

Fig. 2 Diagram of the gap junction synapse. V1 and V2 are the pre- and post- synaptic neuron membrane voltages

We vary the synaptic conductance by varying the values of V_{max}. Theory shows that low values of coupling leads to weaker synchronization between neurons [12]. Thus we use weak coupling strength to prolong the transient time, which implies longer trajectories in the phase lag map. The synaptic conductance is obtained by calculating the slope coefficient in Fig. 3. The value of it is increased by 180% with V_{max} increases from 0.8V to 0.9V.

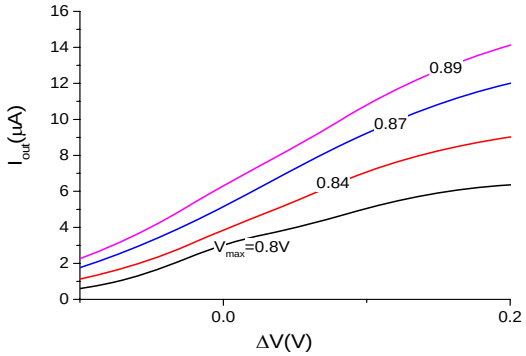

Fig. 3 Output current of the synaptic conductance amplifier as a function of the voltages difference between the pre- and post-synaptic membrane voltages

We use the time delay between the current steps as the parameter that regulates the rhythmic patterns of the neural network (Fig. 4). Step Voltage stimulus is generated by a NI6259 DAQ card and then converted into direct current stimulus by voltage to current converters. Every single neuron is triggered by a current stimulus of 100μA, which is just above the firing threshold of 80μA. The time delay is controlled by the DAQ card. It is varied between 0 and the period of oscillations of the independently firing neuron. If t_n (n=1, 2, 3) is the time when the current step is applied to nth neuron. $\Delta t_1 = t_2 - t_1$, $\Delta t_2 = t_3 - t_2$. We define T_{i1}^n (i=1, 2, 3) as the time position of the nth peak of neuron i relative to the time position of the nth peak of neuron 1. $\Phi_{i1}^n = \frac{T_{i1}^n}{T}$. $\{\Phi_{21}^n, \Phi_{31}^n\}$ is the forward trajectory of the firing sequence. The maps are shown in Figs. 5-8.

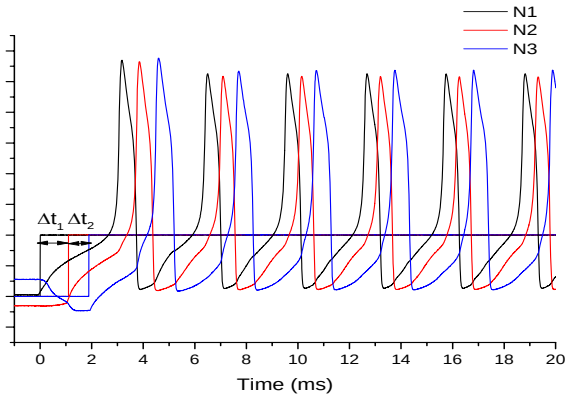

Fig. 4 input current steps are applied to neurons 1, 2 and 3 with offsets of Δt_1 (between N1 and N2) and Δt_2 (between N2 and N3). These delays are varied from 0 to one oscillation period to change the initial conditions of individual oscillators in the CPG. The input current step at 100 μA

III. Results and Discussion

Fig. 5 (a) shows a typical set of neuron oscillations from the time the current stimulus is applied to the time the system

oscillates in the steady-state. These 3 neurons are fired by both direct current injected into the individual neurons and also by the interactions among neurons due to the synaptic connection. The aperiodic oscillations show the dynamics in transient regime. After transient time, the output of the network becomes regular. Fig. 5 (b) is the phase portrait. It shows how the system evolves towards the limit cycle corresponding to the stable spiking patterns.

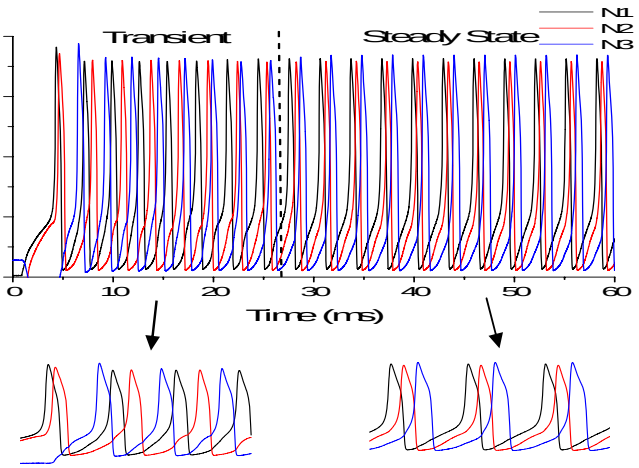

(a)

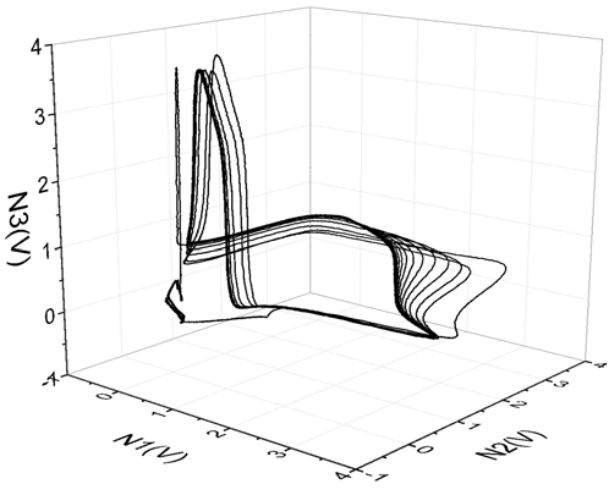

(b)

Fig. 5 (a) Transient oscillations of the coupled neurons evolving towards the steady state. Antiphase oscillations develop in the steady state. (b) Phase portrait of the 3 neuron network from time 0 to 60ms

Fig. 6 shows the $\{\Phi_{21}, \Phi_{31}\}$ phase lag map when the coupling strength g_{12}=g_{23}=g_{13}=16μS, g_{21}=g_{31}=g_{32}=45μS. The conductance is chosen to be asymmetric to prevent the automatic in-phase spiking of neurons [4]. The coupling between neurons is relatively weak in this experiment. There are 2 attraction basins in the map. One attractor is 'a1' at $\{\Delta\Phi_{21} \approx 0.17, \Delta\Phi_{31} \approx 0.36\}$, the other is 'a2' at (0.63, 0.30). (0, 0) is avoided as the neurons cannot fire all in phase due to the asymmetric inhibitory connections. The two basins are divided by a space where there are no trajectories. The trajectory patters are repeatable in other quadrants (not shown in the map).

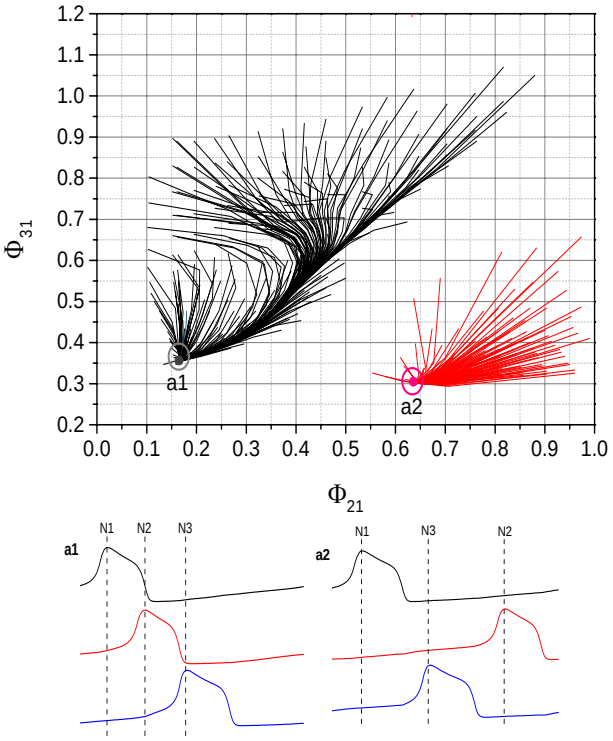

Fig. 6 Top panel: Phase lag map for the synaptic conductance g_{12}=g_{23}=g_{13}=16μS, g_{21}=g_{31}=g_{32}=45μS. 2 attractors are found in the map: a1 (0.17, 0.36); a2 (0.63, 0.3) Bottom panels: rhythmic patterns corresponding to the two attractors

Attractors 'a1' (1→2→3) and 'a2' (1→3→2) represent the clockwise and counterclockwise input injects sequence. Both of the input sequences contribute to trajectories in the left attraction basin. Trajectories in the right attraction basin are caused only by the firing sequence of (1→3→2). Thus the area of the left attraction basin is bigger than the area of the right attraction basin.

Spiking patterns in the bottom panels of Fig. 6 are the steady rhythms produced by the network. Oscillatory modes can be switched from one to another by tuning $(\Delta t_1, \Delta t_2)$.

In Fig. 7 the asymmetry of the mutually inhibitory synaptic couplings is reduced. The synaptic voltage between neurons is g_{12}=35μS, g_{21}=39μS, g_{13}=23.5μS, g_{31}=26μS, g_{23}=22.5μS, g_{32}=39μS. By comparing Fig. 7 with Fig. 6, the longer paths which one observes in the former demonstrate longer transient regimes associated with more symmetric coupling strengths. In Fig. 7 coupling becomes less unidirectional and closer to a mildly chaotic regime. Two attractors are found in the map. They are located at the following coordinates:

$$\{\Delta\Phi_{21} \approx 0.15, \Delta\Phi_{31} \approx 0.55\}$$

and

$$\{\Delta\Phi 21 \approx 0.70, \Delta\Phi 31 \approx 0.35\}.$$

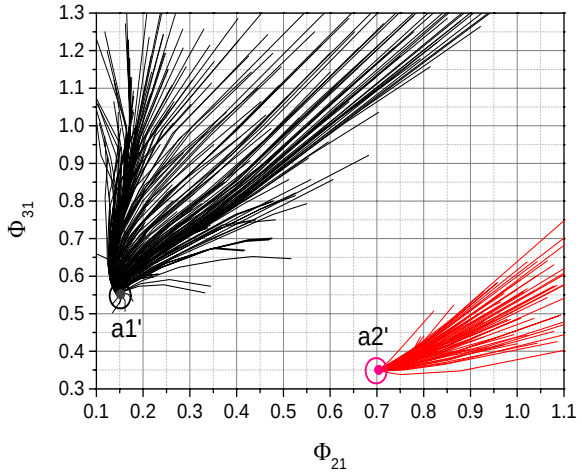

Fig. 7 Phase lag map for the coupling strength g_{12}=35μS, g_{21}=39μS, g_{13}=23.5μS, g_{31}=26μS, g_{23}=22.5μS, g_{32}=39μS. 2 attractors are found in the map: a1' (0.15, 0.55); a2' (0.70, 0.35)

In Fig. 8, we slow down the firing rate of the neurons from 714Hz to 357Hz to study the effect of changing the firing frequency on the phase lag map. Comparison of Figs. 8 and 7 demonstrates that slowing down the neurons leads to better resolution of the separation between attraction basins. The positions of the attractors didn't change.

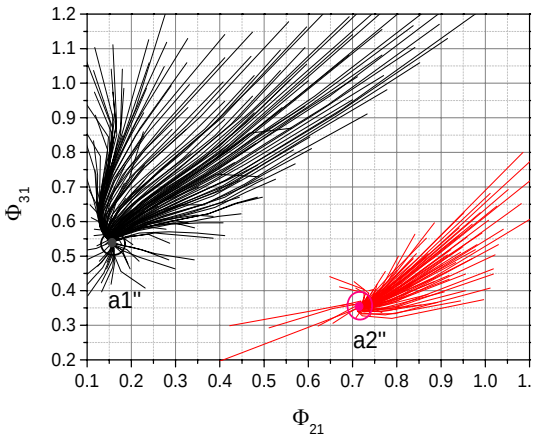

Fig. 8 The coupling strengths are the same with as those in Fig. 7. Frequencies of the individual neurons are reduced from 714Hz to 357Hz by doubling the membrane capacitance of the neurons. Attractors a1'' (0.15, 0.55); a2'' (0.70, 0.35)

IV. Conclusion

We have demonstrated multistable dynamics in a neural network with three analogue neurons coupled by inhibitory synapses. The network supports two distinct stable rhythmic spiking patterns. It is shown that the rhythms can be switched by varying the delayed time of the input current steps. The changing in coupling strengths changes the lengths of trajectories and the positions of the attractors in the phase lag map. Reducing the frequency of individual neurons leads to better resolution of the separation between attraction basins.

References

[1] A. Hess, L.C.Yu, I. klein, M. De Mazancourt, G. Jebrak, H. Mal, O. Brugiere, M. Fournier, M. Courbage, G. Dauriat, E. Schouman-Clayes, C. Clerici, L. Mangin, "Neural mechanisms Underlying Beathing Complexiy", PLoS ONE 8, e7740(2013).
[2] O. Kiehn, Ann. "Locomotor circuits in the mammalian spinal cord", Rev. Neurosci. 29, 279 (2006).
[3] E. Marder, and R. L. Calabrese, "Principles of rhythmic motor pattern generation" Physiol. Rev. 76, 687 (1996).
[4] M. I. Rabinovich, P. Varona, A. I. Selverston, H. D. I. Abarbanel, "Dynamical principles in neuroscience", Rev. Mod. Phys. 78, 1213 (2006).
[5] A. J. Ijspeert, "Central pattern generator for locomotion control in animals and robots: A reveiw", Neural Networkds 21, 642 (2008).
[6] S. Grillner, "Biological pattern generation: The cellular and computational logic of networkds in motion", Neuron 52, 751 (2006).
[7] J. Wojcik, R. Clewley, and A. Shilnikov, "Order parameter for bursting polyrhythms in multifunctional central pattern generators", Phys. Rev, E 83, 056209 (2011).
[8] M. Mahowald, and R. Douglas, "A silicon neuron", Nature 354, 515 (1991).
[9] M. Rabinovich, A. Volkovskii, P. Lecanda, R. Huerta, H.D.I.Abarbanel, "Dynamical encoding by networks of competing neuron groups: Winnerless competition", Phys Rev Lett 87, 068102 (2001).
[10] G. Laurent, M. Stopfer, R. W. friedrich, M. I. Rabinovich, A. Volkovskii, H.D. I. Abarbanel, "Odor encoding as an active, dynamical process: Experiments, computation, and theory", Ann. Rev. Neurosci. 24, 263 (2001).
[11] R. Latorre, C. Aguirre, M. I Rabinovich, P. Varona, "Transient dynamics and rhythm coordination of inferior olive spatio-temporal patterns", Front. Neur. Circ. 7, 138 (2013).
[12] M. Dhamala, V. K. Jirsa, and M. Z. Ding, "Transitions to synchrony in coupled bursting neurons", Phys. Rev. Lett. 92, 074104 (2004).
[13] A. Nogaret, L. Zhao, D.J.A. Moraes, "Modulation of respiratory sinus arrhythmia in rats with central pattern generator hardware", J. Paton, *J. NeuroSci. Meth.* 212, 124 (2013).
[14] A.V.M. Herz, T. Gollisch, C.K. Machens, D. Jaeger, "Modeling single-neuron dynamics and computations: A balance of detail and abstraction", *Science* **314**, 80 (2006).
[15] A. L. Hodgkin and A. F. Huxley, "A quantitative description of membrane current and its application to conduction and excitation in nerve", J. Physiol. 117, 500-544 (1952).